

Measurement of the partial width of the decay of the Z^0 into charm quark pairs

DELPHI Collaboration

P. Abreu ^a, W. Adam ^b, F. Adami ^c, T. Adye ^d, G.D. Alekseev ^e, P. Allen ^f, S. Almedhed ^g, F. Alted ^f, S.J. Alvsvaag ^h, U. Amaldi ⁱ, E. Anassontzis ^j, W.-D. Apel ^k, B. Asman ^l, P. Astier ^m, J.-E. Augustin ⁿ, A. Augustinus ⁱ, P. Baillon ⁱ, P. Bambade ⁿ, F. Barao ^a, G. Barbiellini ^o, D.Y. Bardin ^e, A. Baroncelli ^p, O. Barring ^g, W. Bartl ^b, M.J. Bates ^q, M. Baubillier ^m, K.-H. Becks ^r, C.J. Beeston ^q, P. Beilliere ^s, I. Belokopytov ^t, P. Beltran ^u, D. Benedic ^v, J.M. Benlloch ^f, M. Berggren ^l, D. Bertrand ^w, S. Biagi ^x, F. Bianchi ^y, J.H. Bibby ^q, M.S. Bilenky ^e, P. Billoir ^m, J. Bjarne ^g, D. Bloch ^v, P.N. Bogolubov ^e, D. Bollini ^z, T. Bolognese ^c, M. Bonapart ^{aa}, M. Bonesini ^{ab}, P.S.L. Booth ^x, M. Boratav ^m, P. Borgeaud ^c, H. Borner ^q, C. Bosio ^p, O. Botner ^{ac}, B. Bouquet ⁿ, M. Bozzo ^{ad}, S. Braibant ⁱ, P. Branchini ^p, K.D. Brand ^r, R.A. Brenner ^{ae}, C. Bricman ^w, R.C.A. Brown ⁱ, N. Brummer ^{aa}, J.-M. Brunet ^s, L. Bugge ^{af}, T. Buran ^{af}, H. Burmeister ⁱ, J.A.M.A. Buytaert ^w, M. Caccia ^{ab}, M. Calvi ^{ab}, A.J. Camacho Rozas ^{ag}, J.-E. Campagne ⁱ, A. Champion ^x, T. Camporesi ⁱ, V. Canale ^p, F. Cao ^w, L. Carroll ^x, C. Caso ^{ad}, E. Castelli ^o, M.V. Castillo Gimenez ^f, A. Cattai ⁱ, F.R. Cavallo ^z, L. Cerrito ^p, P. Charpentier ⁱ, P. Checchia ^{ah}, G.A. Chelkov ^e, L. Chevalier ^c, P. Chliapnikov ^t, V. Chorowicz ^m, R. Cirio ^y, M.P. Clara ^y, J.L. Contreras ^f, R. Contri ^{ad}, G. Cosme ⁿ, F. Couchot ⁿ, H.B. Crawley ^{ai}, D. Crennell ^d, M. Cresti ^{ah}, G. Crosetti ^{ad}, N. Crosland ^q, M. Crozon ^s, J. Cuevas Maestro ^{ag}, S. Czellar ^{ae}, S. Dagoret ⁿ, E. Dahl-Jensen ^{aj}, B. Dalmagne ⁿ, M. Dam ⁱ, G. Damgaard ^{aj}, G. Darbo ^{ad}, E. Daubie ^w, P.D. Dauncey ^q, M. Davenport ⁱ, P. David ^m, A. De Angelis ^o, M. De Beer ^c, H. De Boeck ^w, W. De Boer ^k, C. De Clercq ^w, M.D.M. De Fez Laso ^f, N. De Groot ^{aa}, C. De La Vaissiere ^m, B. De Lotto ^o, A. De Min ^{ab}, C. Defoix ^s, D. Delikaris ⁱ, P. Delpierre ^s, N. Demaria ^y, L. Di Ciaccio ^p, A.N. Diddens ^{aa}, H. Dijkstra ⁱ, F. Djama ^v, J. Dolbeau ^s, O. Doll ^r, K. Doroba ^{ak}, M. Dracos ^v, J. Drees ^r, M. Dris ^{al}, W. Dulinski ^v, R. Dzhelyadin ^t, D.N. Edwards ^x, L.-O. Eek ^{ac}, P.A.-M. Eerola ^{ae}, T. Ekelof ^{ac}, G. Ekspong ^l, J.-P. Engel ^v, V. Falaleev ^t, A. Fenyuk ^t, M. Fernandez Alonso ^{ag}, A. Ferrer ^f, S. Ferroni ^{ad}, T.A. Filippas ^{al}, A. Firestone ^{ai}, H. Foeth ⁱ, E. Fokitis ^{al}, F. Fontanelli ^{ad}, H. Forsbach ^r, B. Franek ^d, K.E. Fransson ^{ac}, P. Frenkiel ^s, D.C. Fries ^k, A.G. Frodesen ^h, R. Fruhwirth ^b, F. Fulda-Quenzer ⁿ, H. Furstenau ^k, J. Fuster ⁱ, J.M. Gago ^a, G. Galeazzi ^{ah}, D. Gamba ^y, J. Garcia ^{ag}, U. Gasparini ^{ah}, P. Gavillet ⁱ, S. Gawne ^x, E.N. Gazis ^{al}, J.P. Gerber ^v, P. Giacomelli ^z, K.-W. Glitza ^r, R. Gokieli ^m, V.M. Golovatyuk ^e, A. Goobar ^l, G. Gopal ^d, M. Gorski ^{ak}, Y. Gouz ^t, V. Gracco ^{ad}, A. Grant ⁱ, F. Grard ^w, E. Graziani ^p, I.A. Gribsaenko ^t, M.-H. Gros ⁿ, G. Grosdidier ⁿ, B. Grossetete ^m, S. Gumenyuk ^t, J. Guy ^d, F. Hahn ^r, M. Hahn ^k, S. Haider ⁱ, Z. Hajduk ^{aa}, A. Hakansson ^g, A. Hallgren ^{ac}, K. Hamacher ^r, G. Hamel De Monchenault ^c, F.J. Harris ^q, B. Heck ⁱ, I. Herbst ^r, J.J. Hernandez ^f, P. Herquet ^w, H. Herr ⁱ, E. Higon ^t, H.J. Hilke ⁱ, S.D. Hodgson ^q, T. Hofmokl ^{ak}, R. Holmes ^{ai}, S.-O. Holmgren ^l, J.E. Hooper ^{aj}, M. Houlden ^x, J. Hrubec ^b, P.O. Hulth ^l, K. Hultqvist ^l, D. Husson ^v, B.D. Hyams ⁱ, P. Ioannou ^j, P.-S. Iversen ^h, J.N. Jackson ^x, P. Jalocho ^{am}, G. Jarlskog ^g, P. Jarry ^c, B. Jean-Marie ⁿ, E.K. Johansson ^l, M. Jonker ⁱ, L. Jonsson ^g, P. Juillot ^v, R.B. Kadyrov ^e, G. Kalkanis ^j, G. Kalmus ^d,

G. Kantardjianⁱ, F. Kapusta^m, P. Kapusta^{am}, S. Katsanevas^j, E.C. Katsoufis^{al}, R. Keranen^{ac}, J. Kesteman^w, B.A. Khomenko^e, B. King^x, N.J. Kjaer^{aj}, H. Kleinⁱ, W. Klemptⁱ, A. Klovning^h, P. Kluit^w, J.H. Koehne^k, B. Koene^{aa}, P. Kokkinias^u, M. Kopf^k, M. Koratzinosⁱ, K. Korcyl^{am}, A.V. Korytov^e, B. Korzenⁱ, M. Kostrikov^t, C. Kourkoumelis^j, T. Kreuzberger^b, J. Krolikowski^{ak}, U. Kruener-Marquis^r, W. Krupinski^{am}, W. Kucewicz^{ab}, K. Kurvinen^{ac}, M.I. Laakso^{ae}, C. Lambropoulos^u, J.W. Lamsa^{ai}, L. Lanceri^o, V. Lapin^t, J.-P. Laugier^c, R. Lauhakangas^{ac}, P. Laurikainen^{ac}, G. Leder^b, F. Ledroit^s, J. Lemonne^w, G. Lenzen^r, V. Lepeltierⁿ, A. Letessier-Selvon^m, E. Lieb^r, E. Lillestolⁱ, E. Lillethun^h, J. Lindgren^{ac}, I. Lippi^{ah}, R. Llosa^f, M. Lokajicek^c, J.G. Loken^q, M.A. Lopez Aguera^{ag}, A. Lopez-Fernandezⁿ, D. Loukas^u, J.J. Lozano^f, R. Lucock^d, B. Lund-Jensen^{ac}, P. Lutz^s, L. Lyons^q, G. Maehlumⁱ, N. Magnussen^r, J. Maillard^s, A. Maltezos^u, F. Mandl^b, J. Marco^{ag}, J.-C. Marinⁱ, A. Markou^u, L. Mathis^s, F. Matorras^{ag}, C. Matteuzzi^{ab}, G. Matthiae^p, M. Mazzucato^{ah}, M. Mc Cubbin^x, R. Mc Kay^{ai}, E. Menichetti^y, C. Meroni^{ab}, W.T. Meyer^{ai}, W.A. Mitaroff^b, G.V. Mitselmakher^e, U. Mjoernmark^g, T. Moa^l, R. Moeller^{aj}, K. Moenig^r, M.R. Monge^{ad}, P. Morettini^{ad}, H. Mueller^k, H. Mullerⁱ, G. Myatt^q, F. Naraghi^m, U. Nau-Korzen^r, F.L. Navarria^z, P. Negri^{ab}, B.S. Nielsen^{aj}, V. Nikolaenko^t, V. Obraztsov^t, R. Orava^{ac}, A. Ostankov^t, A. Ouraou^c, R. Pain^m, H. Palka^{am}, T. Papadopoulou^{al}, L. Papeⁱ, A. Passeri^p, M. Pegoraro^{ah}, V. Perevozchikov^t, M. Pernicka^b, A. Perrotta^z, M. Pimenta^a, O. Pingot^w, C. Pinori^{ah}, A. Pinsent^q, M.E. Pol^a, G. Polok^{am}, P. Poropat^o, P. Privitera^z, A. Pullia^{ab}, J. Pyyhtia^{ae}, A.A. Rademakers^{aa}, D. Radojicic^q, S. Ragazzi^{ab}, W.H. Range^x, P.N. Ratoff^q, A.L. Read^{af}, N.G. Redaelli^{ab}, M. Regler^b, D. Reid^x, P.B. Renton^q, L.K. Resvanis^j, F. Richardⁿ, J. Ridky^e, G. Rinaudo^y, I. Roditiⁱ, A. Romero^y, P. Ronchese^{ah}, E.I. Rosenberg^{ai}, U. Rossi^z, E. Rossoⁱ, P. Roudeauⁿ, T. Rovelli^z, V. Ruhlmann^c, A. Ruiz^{ag}, H. Saarikko^{ac}, Y. Sacquin^c, E. Sanchez^f, J. Sanchez^f, E. Sanchis^f, M. Sannino^{ad}, M. Schaeffer^y, H. Schneider^k, F. Scuri^o, A. Sebastia^f, A.M. Segar^q, R. Sekulin^d, M. Sessa^o, G. Sette^{ad}, R. Seuffert^k, R.C. Shellardⁱ, P. Siegrist^c, S. Simonetti^{ad}, F. Simonetto^{ah}, A.N. Sissakian^e, T.B. Skaali^{af}, J. Skeens^{ai}, G. Skjevling^{af}, G. Smadja^c, N.E. Smirnov^t, G.R. Smith^d, R. Sosnowski^{ak}, K. Spang^{aj}, T. Spassoff^e, E. Spiriti^p, S. Squarcia^{ad}, H. Staeck^r, C. Stanescu^p, G. Stavropoulos^u, F. Stichelbaut^w, A. Stocchi^{ab}, J. Strauss^b, R. Strub^y, C.J. Stubenrauchⁱ, M. Szczekowski^{ak}, M. Szeptycka^{ak}, P. Szymanski^{ak}, S. Tavernier^w, G. Theodosiou^u, A. Tilquin^s, J. Timmermans^{aa}, V.G. Timofeev^e, L.G. Tkatchev^e, D.Z. Toet^{aa}, A.K. Topphol^h, L. Tortora^p, M.T. Trainor^q, D. Treilleⁱ, U. Trevisan^{ad}, G. Tristram^s, C. Troncon^{ab}, A. Tsirouⁱ, E.N. Tsyganov^e, M. Turala^{am}, R. Turchetta^y, M.-L. Turluer^c, T. Tuuva^{ae}, I.A. Tyapkin^e, M. Tyndel^d, S. Tzamariasⁱ, F. Udo^{aa}, S. Ueberschaer^r, V.A. Uvarov^t, G. Valenti^z, E. Vallazza^y, J.A. Valls Ferrer^f, G.W. Van Apeldoorn^{aa}, P. Van Dam^{aa}, W.K. Van Doninck^w, N. Van Eijndhovenⁱ, C. Vander Velde^w, J. Varela^a, P. Vaz^a, G. Vegni^{ab}, J. Velasco^f, L. Ventura^{ah}, W. Venus^d, F. Verbeure^w, L.S. Vertogradov^e, L. Vibert^m, D. Vilanova^c, N.K. Vishnevskiy^t, E.V. Vlasov^t, A.S. Vodopyanov^e, M. Vollmer^r, G. Voulgaris^j, M. Voutilainen^{ac}, V. Vrba^e, H. Wahlen^r, C. Walck^l, F. Waldner^o, M. Wayne^{ai}, A. Wehr^r, P. Weilhammerⁱ, J. Werner^r, A.M. Wetherellⁱ, J.H. Wickens^w, J. Wikne^{af}, G.R. Wilkinson^q, W.S.C. Williams^q, M. Winter^y, D. Wormald^{af}, G. Wormserⁿ, K. Woschnagg^{ac}, N. Yamdagni^l, P. Yepes^{aa}, A. Zaitsev^t, A. Zalewska^{am}, P. Zalewski^{ak}, P.I. Zarubin^e, E. Zevgolatakos^u, G. Zhang^r, N.I. Zimin^e, R. Zitoun^m, R. Zukanovich Funchal^s, G. Zumerle^{ah} and J. Zuniga^f

^a LIP, Av. Elias Garcia 14 - 1e, P-1000 Lisbon Codex, Portugal

^b Institut für Hochenergiephysik, Österreichische Akademie der Wissenschaften, Nikolsdorfergasse 18, A-1050 Vienna, Austria

^c DPhPE, CEN-Saclay, F-91191 Gif-Sur-Yvette Cedex, France

^d Rutherford Appleton Laboratory, Chilton, Didcot OX11 0QX, UK

- ^c Joint Institute for Nuclear Research, Dubna, Head Post Office, P.O. Box 79, SU-101 000 Moscow, USSR
- ^f Instituto de Fisica Corpuscular (IFIC), Centro Mixto Universidad de Valencia-CSIC, Avda. Dr. Moliner 50, E-46100 Burjassot (Valencia), Spain
- ^g Department of Physics, University of Lund, Sölvegatan 14, S-223 63 Lund, Sweden
- ^h Department of Physics, University of Bergen, Allégaten 55, N-5007 Bergen, Norway
- ⁱ CERN, CH-1211 Geneva 23, Switzerland
- ^j Physics Laboratory, University of Athens, Solonos Street 104, GR-10680 Athens, Greece
- ^k Institut für Experimentelle Kernphysik, Universität Karlsruhe, Postfach 6980, W-7500 Karlsruhe 1, FRG
- ^l Institute of Physics, University of Stockholm, Vanadisvägen 9, S-113 46 Stockholm, Sweden
- ^m LPNHE, Universités Paris VI et VII, Tour 33 (RdC), 4 place Jussieu, F-75230 Paris Cedex 05, France
- ⁿ Laboratoire de l'Accélérateur Linéaire, Université de Paris-Sud, Bâtiment 200, F-91405 Orsay, France
- ^o Dipartimento di Fisica, Università di Trieste and INFN, Via A. Valerio 2, I-34127 Trieste, Italy and Istituto di Fisica, Università di Udine, I-33100 Udine, Italy
- ^p Istituto Superiore di Sanità, Istituto Nazionale di Fisica Nucleare (INFN), Viale Regina Elena 299, I-00161 Rome, Italy and Dipartimento di Fisica, Università di Roma II and INFN, Tor Vergata, I-00173 Rome, Italy
- ^q Nuclear Physics Laboratory, University of Oxford, Keble Road, Oxford OX1 3RH, UK
- ^r Fachbereich Physik, University of Wuppertal, Postfach 100 127, W-5600 Wuppertal 1, FRG
- ^s Laboratoire de Physique Corpusculaire, Collège de France, 11 place M. Berthelot, F-75231 Paris Cedex 5, France
- ^t Institute for High Energy Physics, Serpukhov, P.O. Box 35, SU-142 284 Protvino (Moscow Region), USSR
- ^u Greek Atomic Energy Commission, Nuclear Research Centre Demokritos, P.O. Box 60228, GR-15310 Aghia Paraskevi, Greece
- ^v Division des Hautes Energies, CRN-Groupe DELPHI and LEPsi, B.P. 20 CRO, F-67037 Strasbourg Cedex, France
- ^w Physics Department, Universitaire Instelling Antwerpen, Universiteitsplein 1, B-2610 Wilrijk, Belgium and IIHE, ULB-VUB, Pleinlaan 2, B-1050 Brussels, Belgium and Service de Physique des Particules Élémentaires, Faculté des Sciences, Université de l'Etat Mons, Av. Maistriau 19, B-7000 Mons, Belgium
- ^x Department of Physics, University of Liverpool, P.O. Box 147, Liverpool L69 3BX, UK
- ^y Dipartimento di Fisica Sperimentale, Università di Torino and INFN, Via P. Giuria 1, I-10125 Turin, Italy
- ^z Dipartimento di Fisica, Università di Bologna and INFN, Via Irnerio 46, I-40126 Bologna, Italy
- ^{aa} NIKHEF-H, Postbus 41882, NL-1009 DB Amsterdam, The Netherlands
- ^{ab} Dipartimento di Fisica, Università di Milano and INFN, Via Celoria 16, I-20133 Milan, Italy
- ^{ac} Department of Radiation Sciences, University of Uppsala, P.O. Box 535, S-751 21 Uppsala, Sweden
- ^{ad} Dipartimento di Fisica, Università di Genova and INFN, Via Dodecaneso 33, I-16146 Genoa, Italy
- ^{ae} Department of High Energy Physics, University of Helsinki, Siltavuorenpenger 20 C, SF-00170 Helsinki 17, Finland
- ^{af} Physics Department, University of Oslo, Blindern, N-1000 Oslo 3, Norway
- ^{ag} Facultad de Ciencias, Universidad de Santander, av. de los Castros, E-39005 Santander, Spain
- ^{ah} Dipartimento di Fisica, Università di Padova and INFN, Via Marzolo 8, I-35131 Padua, Italy
- ^{ai} Ames Laboratory and Department of Physics, Iowa State University, Ames IA 50011, USA
- ^{aj} Niels Bohr Institute, Blegdamsvej 17, DK-2100 Copenhagen Ø, Denmark
- ^{ak} Institute for Nuclear Studies, and University of Warsaw, Ul. Hoza 69, PL-00681 Warsaw, Poland
- ^{al} Physics Department, National Technical University, Zografou Campus, GR-15773 Athens, Greece
- ^{am} High Energy Physics Laboratory, Institute of Nuclear Physics, Ul. Kawioru 26 a, PL-30055 Cracow 30, Poland

Received 6 September 1990

A determination of the partial width Γ_{cc} of the Z^0 boson into charm quark pairs is presented, based on a total sample of 36 900 Z^0 hadronic decays measured with the DELPHI detector at the LEP collider. The production rate of $c\bar{c}$ events is derived from the inclusive analysis of charged pions coming from the decay of charmed meson $D^{*+} \rightarrow D^0\pi^+$ and $D^{*-} \rightarrow \bar{D}^0\pi^-$ where the π^\pm is constrained by kinematics to have a low p_T with respect to the jet axis. The probability to procedure these π^\pm from $D^{*\pm}$ decay in $c\bar{c}$ events is taken to be 0.31 ± 0.05 as measured at $\sqrt{s} = 10.55$ GeV. The measured relative partial width $\Gamma_{cc}/\Gamma_h = 0.162 \pm 0.030$ (stat.) ± 0.050 (syst.) is in good agreement with the standard model value of 0.171. Together with our previous measurement of the total hadronic width Γ_h this implies $\Gamma_{cc} = 282 \pm 53$ (stat.) ± 88 (syst.) MeV.

1. Introduction

Measurements of the hadronic and leptonic partial widths of the Z^0 boson have already been reported by the DELPHI Collaboration [1–3]. A more detailed study of the standard model will need a determination of the Z^0 boson decays into all known quark flavours. This paper presents a determination of the cross section ratio

$$R_{cc} = \frac{\sigma(e^+e^- \rightarrow c\bar{c})}{\sigma(e^+e^- \rightarrow \text{hadrons})} \quad \text{at } \sqrt{s} = 91 \text{ GeV}.$$

Charmed mesons are usually identified via the reconstruction of their decay products. However such an identification has an efficiency of only a few per cent due to the small branching ratios involved. Therefore another technique is applied here which has been already used at lower energies [4,5] and which does not require the reconstruction of exclusive final states. It is well suited to our present limited statistics.

The charm quark is known to fragment predominantly into a charmed vector meson D^* which carries a large fraction of the quark energy [5–8]. In the $D^{*+} \rightarrow D^0\pi^+$ decay^{#1}, whose branching ratio is about 50%, the residual energy is 6 MeV and thus the maximum transverse momentum of the π^+ with respect to the D^{*+} is only 40 MeV/c. Due to the relative transverse momentum of the D^{*+} with respect to the charm quark and due to the smearing in the charm quark jet reconstruction, the mean transverse momentum p_T of the π^+ with respect to its jet axis will be around 65 MeV/c whereas it is about 300 MeV/c for ordinary hadrons in the fragmentation of the jet.

For this reason the p_T^2 distribution of charged particles relative to the jet axis will exhibit an accumulation of events at low transverse momentum which is characteristic of the decay of charmed meson $D^{*+} \rightarrow D^0\pi^+$ in $c\bar{c}$ events. Taking the probability for a charm quark to fragment into a D^{*+} from a measurement at $\sqrt{s} = 10.55$ GeV [6], and assuming this is unchanged at 91 GeV we shall derive the ratio R_{cc} . This assumption is in accord with another measurement at $\sqrt{s} = 29$ GeV [8] and with Lund model predictions.

^{#1} Throughout the paper charge-conjugate states are implicitly included.

2. The DELPHI detector

The components of the apparatus relevant for the present analysis have already been described in refs. [1,2]. Some of its main features are recalled here. The charged particles are measured in a 1.2 T magnetic field (0.7 T for 14% of the total data sample) by a set of three cylindrical tracking detectors: the Inner Detector (ID) covers radii from 12 to 28 cm, the Time Projection Chamber (TPC) from 30 to 122 cm, and the Outer Detector (OD) from 198 to 206 cm. For track reconstruction in the TPC, at least four space points are available for polar angles between 21° and 159° , and up to sixteen space points between 39° and 141° .

In the Barrel part, covering polar angles between 40° and 140° , the trigger on hadronic events is made of redundant subtriggers based on the ID and OD chambers, and on the scintillation counters of the HPC (High density Projection Chamber) and ToF (Time of Flight). The trigger efficiency was found to be larger than 99.9% for hadronic events with a sphericity axis between 50° and 130° . In the forward region, covering polar angles between 15° and 35° and between 145° and 165° , the number of Z^0 events was enhanced by also triggering on an energy deposition of at least 3 GeV in each endcap of the FEMC (Forward Electromagnetic Calorimeter).

3. Event selection

This analysis relies only on tracks from charged particles, using all the data collected from September 1989 up to May 1990 during the three scanning periods around the Z^0 peak (the mean center-of-mass energy was 91 GeV). Charged particles were selected as in refs. [1,2]:

- polar angle θ between 20° and 160° ;
- momentum p between 0.1 GeV/c and 50 GeV/c;
- track length above 30 cm;
- relative error on momentum measurement below 100%;
- projection of impact parameter below 4 cm in the plane transverse to the beam direction;
- distance from the origin below 10 cm along the beam direction.

Hadronic events were retained if they had at least

five charged particles and if the invariant mass of all charged particles was larger than $12 \text{ GeV}/c^2$. These requirements keep 92% of hadronic decays of the Z^0 and reduce any background to a negligible level. The resulting data sample corresponds to 10 100 (26 800) hadronic Z^0 's accumulated in 1989 (1990), the integrated luminosity being 540 (1200) nb^{-1} respectively.

A detailed and reliable simulation is essential in order to establish the selection efficiency for charm quark final states. The quark fragmentation is based on the Lund parton shower model (version Jetset 6.3) [9]. The Monte Carlo simulation of the detector itself includes secondary interactions and collection of electronic signals, allowing the generated events to be treated in the same analysis chain as the real data. We have shown that this simulation describes the distribution of various topological variables of our hadronic data well [10].

Background to π^+ mesons from $D^{*+} \rightarrow D^0\pi^+$ decays in $c\bar{c}$ events comes from all other processes giving low p_T particles with respect to their jet axis. Charmed D^{*+} mesons coming from the decay of bottom hadrons have a lower momentum than those originating from the primordial charm quark. Photons from π^0 decays can convert inside the detector and the electrons from pairs have a low p_T at low momentum. But above an energy of about 1 GeV, the simulation shows that their average p_T is around 200 MeV/c which is close to the p_T of ordinary hadrons.

Charged particles are clustered into jets by using the standard LUCCLUS algorithm of the Lund package [9]. The jet axis is not defined as the sum of momenta of all charged particles in this jet, but as the thrust axis of the jet computed with momentum squared weight [4]. Simulation showed that this definition increases the low p_T π^+ signal to noise ratio by about 20%.

In order to enhance the signal of π^+ mesons from D^{*+} decays, charged particles were retained if they had:

- momentum p between 1.5 and 2.5 GeV/c;
- projection of impact parameter below 2 cm in the plane transverse to the beam direction.

The jet they belonged to had then to satisfy the following requirements:

- at least three charged particles inside the jet;

- at least one particle inside the jet with a momentum larger than p ;

- polar angle of jet axis fulfilling $|\cos \theta_{\text{jet}}| < 0.8$;

- ratio $Z_{\text{jet}} = E_{\text{jet}}/E_{\text{hemi}} > 0.9$;

where E_{jet} and E_{hemi} are respectively the total energy of the jet and the sum of the energies of all charged particles in the same sphericity hemisphere.

The 1.5 GeV/c momentum cut reduces background from $b\bar{b}$ production, photon conversion and particles from soft fragmentation. Few π^+ mesons from D^{*+} decay are expected above 2.5 GeV/c. The cut on the impact parameter reduces the remaining e^\pm contamination. The cuts on the multiplicity inside the jet and on the jet axis direction restrict consideration to jets in which the charged particles are well measured. The cut on Z_{jet} is intended to remove jets from gluon radiation and to enhance the signal from the primary charm quark.

4. Analysis of the p_T^2 distributions

The previous cuts were applied to a Monte Carlo simulation of 34 500 $q\bar{q}$ events. The p_T^2 distribution of charged particles with respect to their jet axis is presented in fig. 1a for $c\bar{c}$ events and in fig. 1b for other $q\bar{q}$ events (where q stands for u, d, s or b quark flavours). The $c\bar{c}$ sample shows a clear accumulation of events with low p_T^2 , not apparent in the non-charm sample. According to the simulation, the contribution of low p_T^2 charged particles from $b\bar{b}$ production happens to be compensated by a depletion in the p_T^2 distribution associated to light quark pairs. This remark applies in particular to the π^\pm produced in the decay of $D^{*\pm}$ originating from beauty hadrons. It reflects a slightly worse angular reconstruction of the jet axis, as defined in section 3, in the case of u, d, s type quarks.

The amount of $D^{*+} \rightarrow D^0\pi^+$ decays contributing to fig. 1a was evaluated as follows:

- first the p_T^2 distribution of the π^+ from $D^{*+} \rightarrow D^0\pi^+$ decay in $c\bar{c}$ events (hatched area in fig. 1a) was fitted for $p_T^2 < 0.01 \text{ (GeV}/c)^2$ with a simple exponential:

$$S(p_T^2) \sim (N_0^q/B^2) \exp(-p_T^2/B^2),$$

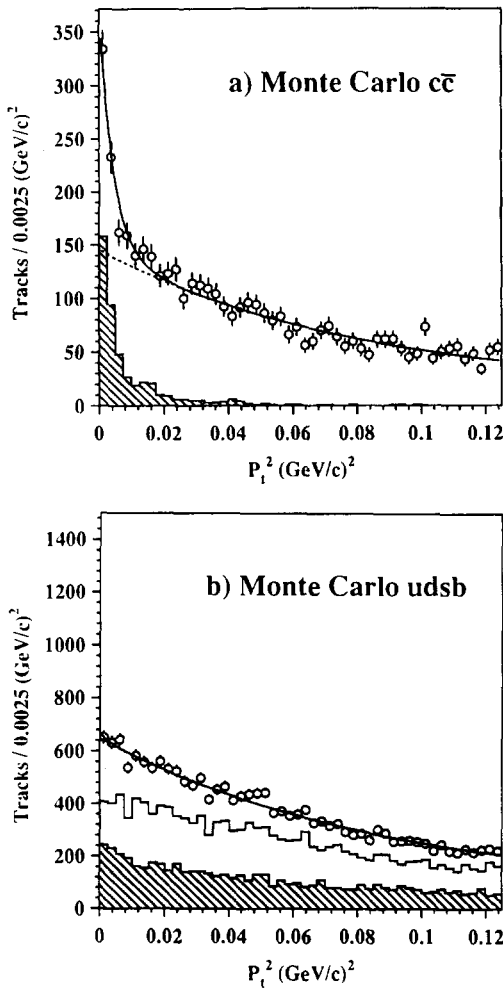


Fig. 1. p_T^2 distribution of charged particles with respect to their jet axis for a Monte Carlo simulation of 34 500 $q\bar{q}$ events after the cuts specified in the text. Curves are the result of a fit $S(p_T^2) + F_1(p_T^2)$ performed for $p_T^2 < 0.25$ $(\text{GeV}/c)^2$ (full line) and the extrapolation of $F_1(p_T^2)$ (dashed line). The simulation is performed (a) for $c\bar{c}$ events only, where π^+ from $D^{*+} \rightarrow D^0\pi^+$ and π^- from $D^{*-} \rightarrow \bar{D}^0\pi^-$ decays are presented in the hatched histogram; or (b) for all quark flavours except charm quark, where $u\bar{u} + d\bar{d} + s\bar{s}$ and $b\bar{b}$ contributions are presented in the upper and in the hatched histograms respectively.

with the normalization N_S^0 and the slope B left free, we found $B = 65 \pm 3$ MeV/c and $N_S^0 = 366 \pm 22$ π^\pm tracks;

– with the slope B fixed, the distribution in p_T^2 of the Monte Carlo events were fitted over the range $0 < p_T^2 < 0.25$ $(\text{GeV}/c)^2$ as the sum $S(p_T^2) + F_i(p_T^2)$

where F_i describes the long-range smooth p_T^2 distribution. The sensitivity of the fits to the shape of the full p_T^2 distribution was evaluated by trying the following two functions with three free parameters each:

$$F_1(p_T^2) \sim a + b \exp(-p_T^2/c^2),$$

$$F_2(p_T^2) \sim \frac{a'}{1 + b'p_T^2 + c'p_T^4}.$$

The fit results are illustrated in fig. 1 and in table 1 for our Monte Carlo simulation. Both shapes correctly describe the non-charm $q\bar{q}$ sample without significant signal; for the $c\bar{c}$ sample each fit $S + F_i$ gives an amount of signal N_S in agreement with the value 366 ± 22 expected.

For the selected sample of real data (36 900 hadronic Z^0 events) fig. 2 shows the p_T^2 distributions of charged particles for two momentum intervals:

$$1.5 < p < 2.5 \text{ GeV}/c \text{ (a)},$$

$$3 < p < 4 \text{ GeV}/c \text{ (b)}.$$

At high momentum (b) we see no significant accumulation at low p_T^2 in agreement with the Monte Carlo expectation, while in the momentum range (a) an excess is apparent. Following the same procedure as for Monte Carlo events, the distribution displayed in fig. 2a was fitted for $p_T^2 < 0.25$ $(\text{GeV}/c)^2$ with the shape $S + F_i$ where the slope $B = 65$ MeV/c is fixed and where the three parameters in F_i are left free. This fit yields $N_S = 336 \pm 68$ ($\chi^2/\text{DF} = 125/96$) with F_1 and $N_S = 426 \pm 76$ ($\chi^2/\text{DF} = 128/96$) with F_2 . The average of these two results gives the measured $\pi^+ + \pi^-$ signal: $N_S = 381 \pm 72$, and the observed difference between the two fits is converted into a systematic error of ± 64 due to the uncertainty on the

Table 1

Fits of p_T^2 distributions of simulated events (34 500 generated $q\bar{q}$ events).

Quark flavours	Parametrization	Signal N_S	χ^2/DF
$c\bar{c} \rightarrow D^{*+} \rightarrow D^0\pi^+$	$S(p_T^2)$	366 ± 22	0.34/2
$c\bar{c}$ alone	$S(p_T^2) + F_1(p_T^2)$	392 ± 38	97/96
	$S(p_T^2) + F_2(p_T^2)$	360 ± 45	94/96
all flavours except $c\bar{c}$	$S(p_T^2) + F_1(p_T^2)$	28 ± 60	109/96
	$S(p_T^2) + F_2(p_T^2)$	12 ± 64	110/96

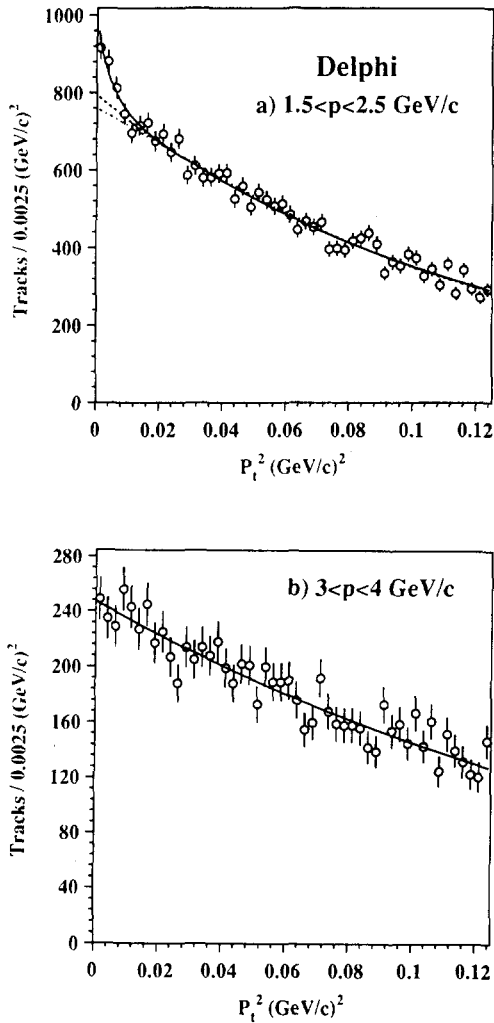


Fig. 2. p_T^2 distribution of charged particles with respect to their jet axis for 36 900 hadronic events detected in DELPHI. Curves are the result of a fit $S(p_T^2) + F_1(p_T^2)$ performed for $p_T^2 < 0.25$ $(\text{GeV}/c)^2$ (full line) and the extrapolation of $F_1(p_T^2)$ (dashed line) or $F_2(p_T^2)$ (dash-dotted line). The momentum of the charged particles is in the range $1.5 < p < 2.5$ GeV/c (a) or $3.0 < p < 4.0$ GeV/c (b).

shape of the background. The signal to noise ratio is about 0.14 in the range $p_T^2 < 0.0075$ $(\text{GeV}/c)^2$.

This method relies on an assumed slope for the expected signal $S(p_T^2)$. Another method is to fix the background F_i by fitting the p_T^2 distribution for p_T^2 above 0.0125 $(\text{GeV}/c)^2$. Then the subtraction of the extrapolated background F_i from the observed num-

Table 2

Experimental value of the signal N_S fitted from the p_T^2 distribution of 36 900 hadronic events, where N_S is quoted for $p_T^2 < 0.0075$ $(\text{GeV}/c)^2$. Due to the exponential shape of the p_T^2 distribution of the expected signal, the integrated signal N_S over the full p_T^2 range is obtained by multiplying N_S by a factor 1.204. The first line shows the values of N_S obtained with the shapes $S(p_T^2) + F_1(p_T^2)$. The next two lines show the difference between the total number of tracks below $p_T^2 < 0.0075$ $(\text{GeV}/c)^2$ and the number given by the extrapolation of the fitted shapes $F_i(p_T^2)$ alone.

p_T^2 range used in the fit $(\text{GeV}/c)^2$	Shape $S(p_T^2) + F_1(p_T^2)$	Shape $S(p_T^2) + F_2(p_T^2)$
0–0.25	279 ± 56	354 ± 63
	Shape $F_1(p_T^2)$ alone	Shape $F_2(p_T^2)$ alone
0.0125–0.25	298 ± 58	376 ± 70
0.025–0.25	310 ± 60	458 ± 84

ber of tracks below 0.0075 $(\text{GeV}/c)^2$ gives an estimate N_S of the signal. The results of this method applied to the real data are summarized in table 2 for different p_T^2 ranges. Extrapolating from p_T^2 larger than 0.0125 $(\text{GeV}/c)^2$, both parametrizations lead to a compatible level of signal below 0.0075 $(\text{GeV}/c)^2$. This holds also for different p_T^2 intervals, especially for the exponential curve F_1 whereas the extrapolation from the inverse of polynomial F_2 presents a larger error. We can conclude that, within statistical errors, the signal shape obtained from Monte Carlo simulation correctly describes real data.

5. Measurement of the $Z^0 \rightarrow c\bar{c}$ relative partial width

The cross section $R_{c\bar{c}} = \sigma(e^+e^- \rightarrow c\bar{c}) / \sigma(e^+e^- \rightarrow \text{hadrons})$ is measured as

$$R_{c\bar{c}} = \frac{\varepsilon_h}{N_h} \times \frac{N_S}{\varepsilon_{c\bar{c}} \times \varepsilon_S}$$

where N_h stands for the number of selected hadronic events ($N_h = 36\,900$), N_S is the number of fitted charged particles in the signal at low p_T^2 ($N_S = 381 \pm 72$), ε_h and $\varepsilon_{c\bar{c}}$ are the overall efficiencies for hadronic and $c\bar{c}$ events, and ε_S stands for the efficiency to count π^+ mesons in $c\bar{c}$ events. With our se-

lection criteria, ε_h and ε_{cc} present no significant difference: $\varepsilon_h/\varepsilon_{cc} = 1.000 \pm 0.005$ from the Monte Carlo simulation. The efficiency ε_s can be expressed as

$$\varepsilon_s = \mathcal{P}_1(c\bar{c} \rightarrow D^{*\pm} + X \text{ with } D^{*\pm} \rightarrow D^0\pi^+) \\ \times \mathcal{P}_2(\pi^+ \text{ as measured}) \times \mathcal{P}_3(\pi^+ \text{ as fitted}),$$

where \mathcal{P}_1 is the probability to produce $D^0\pi^+$ from $D^{*\pm}$ decays in $c\bar{c}$ events, \mathcal{P}_2 is the probability to reconstruct and select a π^+ meson, and \mathcal{P}_3 is the probability to count these measured π^+ in the fitting procedure.

\mathcal{P}_1 can be obtained from a measurement by the CLEO Collaboration [6] at $\sqrt{s} = 10.55$ GeV of the cross section

$$\sigma(e^+e^- \rightarrow D^{*\pm} + X \text{ with } D^{*\pm} \rightarrow D^0\pi^+)$$

and averaging over two decay modes of the D^0 meson (see table 3): $D^0 \rightarrow K^-\pi^+$ and $K^-\pi^+\pi^-\pi^+$ using the branching fractions of the D^0 measured by MARK III [11]. This probability does not depend on a measurement of the branching fraction of the decay $D^{*\pm} \rightarrow D^0\pi^+$, nor on the ratio of vector to pseudo-scalar charmed meson production. Furthermore the above cross section was measured for the continuum with a kinematic constraint forbidding the detection of charmed mesons in $\Upsilon(4S) \rightarrow B\bar{B}$ events. The probability thus obtained is $\mathcal{P}_1 = 0.308 \pm 0.046$ at $\sqrt{s} = 10.55$ GeV, in agreement with the value 0.315 ± 0.046 deduced from the HRS experiment at $\sqrt{s} = 29$ GeV

Table 3

Computation of the probability \mathcal{P}_1 ($c\bar{c} \rightarrow D^{*\pm} + X$ with $D^{*\pm} \rightarrow D^0\pi^+$) from CLEO results at $\sqrt{s} = 10.55$ GeV [6].

$$\mathcal{P}_1 = \frac{\sigma_{D^0}^0}{R_{cc}^0 \times \sigma_h^0} = 0.308 \pm 0.046$$

where

$$R_{cc}^0 = \sigma(e^+e^- \rightarrow c\bar{c}) / \sigma(e^+e^- \rightarrow \text{hadrons}) = 0.37 \pm 0.02 [6]$$

$$\sigma_h^0 = \sigma(e^+e^- \rightarrow \text{hadrons}) = 3.33 \pm 0.05 \pm 0.21 \text{ nb} [6,12]$$

$$\sigma_{D^0}^0 = \sigma(e^+e^- \rightarrow D^* + X \text{ with } D^{*\pm} \rightarrow D^0\pi^+, \text{ or } D^{*\pm} \rightarrow \bar{D}^0\pi^-) \\ = 0.379 \pm 0.046 \text{ nb}$$

$\sigma_{D^0}^0$ is computed from measurements shown below.

Decay mode of D^0	$B \sigma_{D^0}^0$ (pb) ^{a)}	Branching fraction B ^{b)}
$D^0 \rightarrow K^-\pi^+$	$17.0 \pm 1.5 \pm 1.4$	$0.042 \pm 0.004 \pm 0.004$
$D^0 \rightarrow K^-\pi^+\pi^-\pi^+$	$33.0 \pm 3.0 \pm 1.8$	$0.091 \pm 0.008 \pm 0.008$

^{a)} Ref. [6]. ^{b)} Ref. [11].

[8] but where the error on the cross section of $c\bar{c}$ production, including the $b \rightarrow c$ transition, is not quoted. In the following, the value $\mathcal{P}_1 = 0.31 \pm 0.05$ is used, with the assumption that the fragmentation rate of charm into $D^{*\pm}$ does not change from 10.55 up to 91 GeV center-of-mass energy.

The probability \mathcal{P}_2 to reconstruct and select π^+ mesons with our criteria described in section 3, is deduced from the Monte Carlo simulation: $\mathcal{P}_2 = 0.27 \pm 0.02$. The main causes of loss are the momentum selection of π^+ between 1.5 and 2.5 GeV/c and the requirement that the π^+ is inside a jet free from hard gluon radiation. The error takes into account a shift of $\pm 10\%$ in the momentum of the π^+ from the uncertainty in the fragmentation function of the charm quark.

The proportion \mathcal{P}_3 of these π^+ mesons which are finally fitted from the overall p_T^2 distribution is also taken from the simulation $\mathcal{P}_3 = 0.78 \pm 0.05$, where the error reflects an uncertainty of 5% on the slope B of the signal shape.

Finally the important assumption is that the only contribution to the observed accumulation of tracks at low p_T^2 comes from $D^{*\pm} \rightarrow D^0\pi^+$ decays occurring in $c\bar{c}$ events. The background from the other quark flavours, including $b\bar{b}$, is evaluated with the Monte Carlo simulation (table 1) and transforms into an 18% systematic error on the fitted value of N_S . The electron background is negligible within the cuts because, according to the simulation, their p_T^2 slope is large and a variation of $\pm 20\%$ of their amount would change N_S by only $\pm 1\%$.

The resulting cross section ratio is thus

$$R_{cc} = 0.162 \pm 0.030(\text{stat.}) \pm 0.050(\text{syst.}),$$

where the statistical error results from the fitting procedure and where the various contributions to the systematic error are listed in table 4.

The predicted value of the standard model for the ratio of the partial width Γ_{cc} of the Z^0 into $c\bar{c}$ to the total hadronic width Γ_h is [13]

$$\frac{\Gamma_{cc}}{\Gamma_h} = 0.171 \text{ (S.M.)}.$$

Table 4
Contributions to the systematic error on Γ_{cc}/Γ_h .

Contributions	Systematic error
ratio of global efficiencies $\varepsilon_h/\varepsilon_{cc}$	± 0.001
probability ($c\bar{c} \rightarrow D^{*+}$ with $D^{*+} \rightarrow D^0\pi^+$)	± 0.026
reconstruction and selection of π^+ mesons	± 0.012
shape of the signal in fitting procedure	± 0.010
choice of the background shape	± 0.027
background from other quark flavours	± 0.029
electron background	± 0.002
total	± 0.050

6. Conclusion

An inclusive analysis of $Z^0 \rightarrow c\bar{c}$ events has been performed at LEP using the low momentum and low $p_T \pi^\pm$ mesons produced in the decays of charmed mesons $D^{*+} \rightarrow D^0\pi^+$ and $D^{*-} \rightarrow \bar{D}^0\pi^-$. Assuming that in $c\bar{c}$ events the probability of producing such a low momentum π^\pm from $D^{*\pm}$ decays is 0.31 ± 0.05 [6], the partial width ratio is found to be

$$\frac{\Gamma_{cc}}{\Gamma_h} = 0.162 \pm 0.030(\text{stat.}) \pm 0.050(\text{syst.}),$$

in agreement with another measurement [14] and with the standard model prediction of 0.171 [13]. From our previous measurement of the total hadronic width [2],

$$\Gamma_h = 1741 \pm 61 \text{ MeV},$$

we deduce the Z^0 partial width into charm quark pairs:

$$\Gamma_{cc} = 282 \pm 53(\text{stat.}) \pm 88(\text{syst.}) \text{ MeV}.$$

Acknowledgement

We are greatly indebted to our technical staffs and collaborators and funding agencies for their support in building the DELPHI detector and to the members of the LEP Division for the superb performance of the LEP collider.

References

- [1] DELPHI Collab., P. Aarnio et al., Phys. Lett. B 231 (1989) 539.
- [2] DELPHI Collab., P. Abreu et al., Phys. Lett. B 241 (1990) 435.
- [3] DELPHI Collab., P. Aarnio et al., Phys. Lett. B 241 (1990) 425.
- [4] HRS Collab., S. Abachi et al., Phys. Lett. B 205 (1988) 411.
- [5] TASSO Collab., W. Braunschweig et al., Z. Phys. C 44 (1989) 365.
- [6] CLEO Collab., D. Bortoletto et al., Phys. Rev. D 37 (1988) 1719; D 39 (1989) 1471.
- [7] MARK II Collab., J.M. Yelton et al., Phys. Rev. Lett. 49 (1982) 430; JADE Collab., W. Bartel et al., Phys. Lett. B 146 (1984) 121; ARGUS Collab., H. Albrecht et al., Phys. Lett. B 150 (1985) 235; DELCO Collab., H. Yamamoto et al., Phys. Rev. Lett. 54 (1985) 522; TPC/Two-Gamma Collab., H. Aihara et al., Phys. Rev. D 34 (1986) 1945.
- [8] HRS Collab., P. Baringer et al., Phys. Lett. B 206 (1988) 551.
- [9] T. Sjöstrand, Comput. Phys. Commun. 27 (1982) 243; 28 (1983) 229; T. Sjöstrand and M. Bengtsson, Comput. Phys. Commun. 43 (1987) 367.
- [10] DELPHI Collab., P. Aarnio et al., Phys. Lett. B 240 (1990) 271.
- [11] MARK III Collab., J. Adler et al., Phys. Rev. Lett. 60 (1988) 89.
- [12] CLEO Collab., R. Giles et al., Phys. Rev. D 29 (1984) 1285.
- [13] W.F.L. Hollik, DESY preprint DESY 88-188 (1988).
- [14] ALEPH Collab., D. Decamp et al., Phys. Lett. B 244 (1990) 551.